Arabian Journal of Chemistry (2022) **15**, 103765

King Saud University

Arabian Journal of Chemistry

www.ksu.edu.sa
www.sciencedirect.com

ORIGINAL ARTICLE

First report of flavonoids from leaves of *Machaerium acutifolium* by DI-ESI-MS/MS

Adonias Almeida Carvalho [a,b], Lucivania Rodrigues dos Santos [b], Jurema Santana de Freitas [b], Renato Pinto de Sousa [b], Ruth Raquel Soares de Farias [c], Gerardo Magela Vieira Júnior [b], Mahendra Rai [d], Mariana Helena Chaves [b,*]

[a] *Federal Institute of Piauí - Piripiri Campus, 64260-00 Piripiri, Piauí, Brazil*
[b] *Department of Chemistry, Federal University of Piauí, 64049-550 Teresina, Piauí, Brazil*
[c] *bioTEM, Federal University of Piauí, Teresina, Piauí, Brazil*
[d] *Department of Biotechnology, SGB Amravati University, Amravati 444 602, Maharashtra, India*

Received 16 July 2021; accepted 2 February 2022
Available online 7 February 2022

KEYWORDS

Machaerium acutifolium;
HPLC-DAD;
DI-ESI-MS/MS;
Flavonoids;
Isoflavonoids;
Antioxidant activity;
Total phenolic content

Abstract The aqueous fraction obtained by the partition of the ethanolic extract from leaves of *Machaerium acutifolium* (Fabaceae-Papilionoideae) was analyzed by high-performance liquid chromatography with a diode array detector (HPLC-DAD) and direct insertion in a mass spectrometer with an ion trap analyzer equipped with an electrospray ionization source (DI-ESI-MS/MS). The chemical analysis of the extract demonstrated the occurrence of eight flavonols (**1**–**8**), two isoflavonoids (**9** and **10**) and one biflavonoid (**11**). These compounds are being reported for the first time from *M. acutifolium*. The aqueous fraction showed 28.37 ± 0.94% of AA in assay on DPPH and 151.70 ± 9.44 GAE of the total phenolic content.

Abbreviations: HPLC-DAD, high-performance liquid chromatography with diode array detector; HPLC-UV, high-performance liquid chromatography with ultraviolet detection; DI-ESI-MS/MS, direct insertion in a mass spectrometer with an ion trap analyzer equipped with an electrospray ionization source; AA, antioxidant activity; TPC, total phenolic content; GAE, gallic acid equivalent; DPPH, 2,2-diphenyl-1-picrylhydrazyl

* Corresponding author.
E-mail addresses: adonias.carvalho@ifpi.edu.br (A.A. Carvalho), magela@ufpi.edu.br (G.M. Vieira Júnior), mariana@ufpi.edu.br (M.H. Chaves).

Peer review under responsibility of King Saud University.

Production and hosting by Elsevier

https://doi.org/10.1016/j.arabjc.2022.103765

1. Introduction

Machaerium acutifolium Vogel (Fabaceae - Papilionoideae) popularly known as "jacarandá do campo", "jacarandá caroba" and "jacarandá bico de pato", occurs in Brazil, from Amazon, São Paulo, Mato Grosso do Sul, Bahia, Piauí and Maranhão states, mainly in the cerrado area (Lorenzi, 1998; Polido and Sartori, 2007). This plant species is traditionally used as a contraceptive to treat painful menstruation and stomach pain (Barbosa and Pinto, 2003). Ollis et al. (1978) reported that the trunk wood of *M. acutifolium* contains polyphenols (pinsylvin monomethyl ether, (+)-medicarpin, and petrostyrene). A recent study revealed that trunk ethyl acetate extract of *M. acutifolium* contains: one 3-arylcoumarin derivative, two flavonoids: (3*R*)–*2H*-benzopyran-7-ol, 3,4-dihydro-3-(2'hydroxy-3',4'-dimethoxy phenyl) and (*3R*)–*2H*-benzopyran-7-ol, 3,4-dihydro-3-(2'hydr oxy-3',4'-dimethoxyphenyl)-8-methoxy, one *trans*-stilbene and a natural indene (Melo et al., 2021). The authors further confirmed the larvicidal activity of crude extract and natural indene.

HPLC is a fundamental technique for the screening and separation of flavonoids (Pinheiro and Justino, 2012; Carvalho et al., 2018). While mass spectrometry (MS) is widely used to identify these compounds (Prasain et al., 2003; Silva et al., 2021; Zhao et al., 2018). Tandem MS (MS/MS) with electrospray ionization (ESI) interface is a valuable technique for the identification of metabolites, due to the high selectivity and ionic resolution. In recent years, it has been widely used for the identification of structures and in the isomeric differentiation of glycosylated flavonoids (Vukics and Guttman, 2010). Studies have shown that the position of sugar substitution has a significant influence on the fragmentation pattern of *O*-glycosylated flavonoids (Ablajan, 2010; Es-Safi et al., 2005).

Considering the biological importance of *M. acutifolium* and the few previous report, a systematic study was carried out to identify secondary metabolites (flavonoids and isoflavonoids) in the phenolic-rich aqueous fraction, obtained from the leaves of *M. acutifolium* by DI-ESI-MS/MS and NMR, and also to evaluate the antioxidant potential and the total phenolic content. Part of this paper was presented in the form of an abstract at the 7th Brazilian Conference on Natural Products held in Rio de Janeiro, Brazil (Carvalho et al., 2019).

2. Materials and methods

2.1. Plant material

Fresh leaves of *M. acutifolium* were collected from Jatobá do Piauí, state of Piauí, Brazil (S 04° 51 '006″, W 42° 05 '057″, 100 m), in March 2017. The plant was identified by biologist Dr. Ruth R. S. de Farias and a voucher specimen was deposited at the Herbarium Graziela Barroso (Federal University of Piauí - UFPI), under code TEPB 31,568 and SisGen AAB530D.

2.2. Sample preparation

The leaves were air-dried (1.4 kg), pulverized in a mechanical grinder, and exhaustively macerated with ethanol (98%). The solvent was removed in a rotary evaporator under reduced pressure and the residual water by lyophilization, yielding 74.7 g of ethanolic extract (5.3%). The crude extract (64 g) was suspended in methanol–water (1:2, v/v) and partitioned successively with hexane and ethyl acetate that resulted in the hexane (FHF, 33.5 g, 52.3%), ethyl acetate (FAEF, 5 g, 7.8%) and aqueous fractions (FAF, 25.5 g, 39.8%). The aqueous fraction was analyzed by HPLC-DAD and DI-ESI-MS/MS.

2.3. Extraction of phenolic compounds

The fraction rich with phenolic compounds was obtained by solid-phase extraction (SPE) of the aqueous fraction. An aliquot (10 mg) of the aqueous fraction was dissolved in 1 mL of the MeOH/H_2O (1:1, v/v) and applied in SPE cartridge (1.0 × 3.5 cm - Bakerbondspe 7020–03, C18, 25–40 μm, JT Baker), previously conditioned with the same solvent and eluted with 1 mL of MeOH/H_2O (1:1, v/v). The sample was filtered in membrane 0.45 and 0.22 μm (Millipore®) for analysis in HPLC and DI-ESI-MS/MS (50 ppm), respectively.

HPLC analysis were carried out in chromatographs: i) analytical, Shimadzu® equipped with LC-20AT pump, SIL-20AHT automatic injector, SPD-M20A diode array detector, CTO-20A column oven, C18 Shim- pack 6-SIL, column C-18Shim-pack VP-ODS (250 x 4.6 mm, 5 μm) and ii) semi-preparative, Shimadzu® prominence system equipped with LC-6AD binary pump system, manual injector, SPD-20A UV detector, Phenomenex Luna column (C18, 250 x 10 mm, 15 μm). The solvents, (A) H_2O-0.2% AcOH and (B) MeOH, were used as mobile phase, being methanol and acetic acid of grade HPLC (J. T. Backer) and ultra-pure water (18 Ω, Milli-Q Plus system). The column temperature was maintained at 30 °C.

DI-ESI-MS/MS analysis was achieved by direct insertion in a mass spectrometer with an ion trap analyzer (ITMS, AmaZon X, Bruker Daltonics), equipped with an electrospray ionization (ESI) source. The conditions used for the analysis were: ESI ionization source in negative ion mode, [ESI(-)], *m*/*z* range 100–1500, syringe flow 3.0 μL min^{-1}, capillary voltage 4.5 kV, the flow of drying gas (N_2) 9.0 L min^{-1}, nebulization pressure 50 psi and source temperature 350 °C. For MS^n analysis, the parameters collision energy, signal amplitude, data acquisition time, and radiofrequency were adjusted for each signal, in order to obtain structural information from the precursor ion.

2.4. Isolation of major compounds

Seven 500 mg aliquots of the aqueous fraction of the leaves were solubilized in H_2O/MeOH (8:2) with the aid of an ultrasonic bath and applied to a solid-phase extraction cartridge (SPE, C18, 10 g), initially acclimated with H_2O/MeOH (8:2) and eluted successively with 150 mL of each of the following eluents: MeOH/H_2O (8:2), MeOH (100%) and $CHCl_3$ (100%). The corresponding eluates were pooled giving the subfractions R1 (3.1 g, 89.7%), R2 (300.5 mg, 8.6%) and R3 (59.5 mg, 1.7%), respectively.

The R1 subfraction was fractionated on semipreparative HPLC-UV, utilizing the gradient elution: 0–104 min; 30–90% MeOH, injection volume 1 mL, flow rate 4 mL min^{-1}

and λ = 254 nm. The chromatographic separation allowed the isolation of compounds **5** (66.6 mg) and **6** (45.9 mg).

2.5. DPPH assay and determination of total phenolic content

The evaluation of the antioxidant activity (AA) of the aqueous fraction of the leaves was made by the spectrophotometric method based on the DPPH free radical scavenging (Sousa et al., 2007).

A stock solution of DPPH, with a concentration of 40 μg mL^{-1} was prepared and kept under refrigeration and protected from light. The flavonoid rutin and the synthetic compound butylhydroxytoluene (BHT) were used as a positive control. A 250 μg mL^{-1} stock solution was prepared in triplicate and diluted to concentrations of 200, 150, 100, 50, and 25 μg mL^{-1}. The absorbance measurements of the reaction mixtures (0.3 mL of the sample solution and 2.7 mL of the DPPH stock solution, at a concentration of 40 μg mL^{-1}), were taken at 516 nm, in triplicate, on the 1st, 5th, and 10th minute of analysis, every 10 min until completing 30 min. A mixture of methanol (2.7 mL) and methanol sample solution (0.3 mL) was used as blank. The equation of the analytical curve used to determine the concentration of DPPH was $A = 33.227c + 1.0607$, with a linear correlation coefficient R = 0.9997, where "c" equals the concentration of DPPH in the reaction medium and "A" is the absorbance obtained at the wavelength (λ_{max}) of 516 nm. From the equation of the analytical curve of DPPH and the absorbance values in a time of 30 min for each concentration tested, the percentage of remaining DPPH (%$DPPH_{rem}$) and the percentage of AA were determined.

The percentage of antioxidant activity (%AA) was determined from the absorbance values of the samples measured at concentrations of 25, 50, 100, 150, 200, and 250 μg mL^{-1} in a time of 30 min, using Equation (1) where: Abs_{DPPH} is the initial absorbance of the DPPH solution, Abs_{sample} is the absorbance of the reaction mixture and Abs_{blank} is the absorbance of the blank.

$$\%AA = \{[Abs_{DPPH} - (Abs_{sample} - Abs_{blank})/Abs_{DPPH}]\} \times 100 \quad (1)$$

To determine the percentage of remaining or residual DPPH (%$DPPH_{rem}$) we used Equation (2).

$$\%\boldsymbol{DPPH_{rem}} = (\boldsymbol{DPPH_{t=30}}/\boldsymbol{DPPH_{t=0}}) \times 100 \quad (2)$$

The efficient concentration of the extract capable of reducing the DPPH free radical concentration by 50% (EC_{50}) in μg mL^{-1} was also determined from the first-order exponential curve of %$DPPH_{rem}$ versus the sample concentrations (Sousa et al, 2007).

The total phenolic content (TPC) of the aqueous fraction of the leaves was determined by spectrometry in the visible region using the Folin-Ciocalteu method as described by Sousa et al. (2007), analyses performed in triplicate. Aqueous sodium carbonate (15%) and methanolic solution of sample, at a concentration of 1.0 mg L^{-1}, were prepared and stored. 500 μL of Folin-Ciocalteu reagent was added to an aliquot of 100 μL of the sample solution, followed by 5.0 mL of distilled water and stirred for one minute. Then, 2.0 mL of sodium carbonate solution (15%) was added to the reaction mixture, stirring for 30 s, the volume of 10 mL was made up with distilled water, allowed to react for two hours, and measured the absorbance at a wavelength of 750 nm. For the blank, the same procedure was performed, replacing the sample solution with 100 μL of methanol.

The determination of TPC levels was made by interpolating the absorbance of the samples against an analytical curve constructed with a standard of gallic acid (10 to 350 μg mL^{-1}) and expressed as $A = 0.1185c–0.0453$, with a correlation coefficient linear equal to 0.999, where "c" is the concentration of gallic acid and "A" is the absorbance. TPC was expressed in milligrams of gallic acid equivalent per gram of extract (mg EAG g^{-1}).

2.6. Statistical analysis

The results presented in this study correspond to the average of three repetitions (n = 3) ± standard deviation of the mean. The results of antioxidant activity that presented a probability of occurrence of the null hypothesis lower than 5% ($p < 0.05$) were considered statistically different, applying ANOVA, followed by multiple comparisons using the Tukey test. All analyses were performed using the *Microcal Origin 8.0* software.

3. Results and discussions

The chromatographic profile of the aqueous fraction obtained from the ethanol extract partition showed two intense peaks (Fig. 1). The spectra in the UV region corresponding to these peaks showed absorptions between 300 and 380 and 240 to 280, referring to the cinnamoyl (band I) and benzoyl (band II) systems, respectively (Mabry et al., 1970).

The aqueous fraction rich in phenolic compounds, obtained in a solid-phase extraction cartridge (SPE, C18, 10 g), was applied in semipreparative HPLC, allowing the isolation of major compounds **5** (t_R = 9.99) and **6** (t_R = 15.44). These compounds were identified by DI-ESI-MS/MS, ^1H and ^{13}C NMR and comparison with literature data (Kite et al., 2007; Silva et al., 2018).

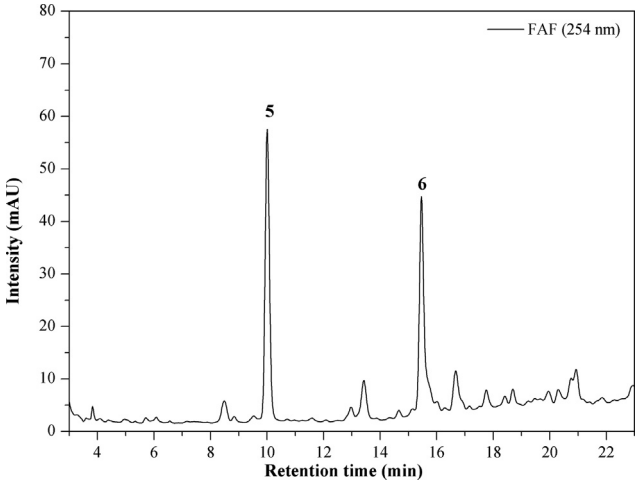

Fig. 1 Chromatogram of aqueous fraction. Mobile Phase: MeOH/H_2O-AcOH (0.2%), gradient: 0-5min, 30-40% MeOH; 5-7min, 40% MeOH; 7-12min, 40-50% MeOH; 12-14min, 50% MeOH; 14-19min, 50-60% MeOH; 19-23min, 60-100% MeOH, injection volume 10 μL, flow rate 1 mL min^{-1} and λ = 254 nm.

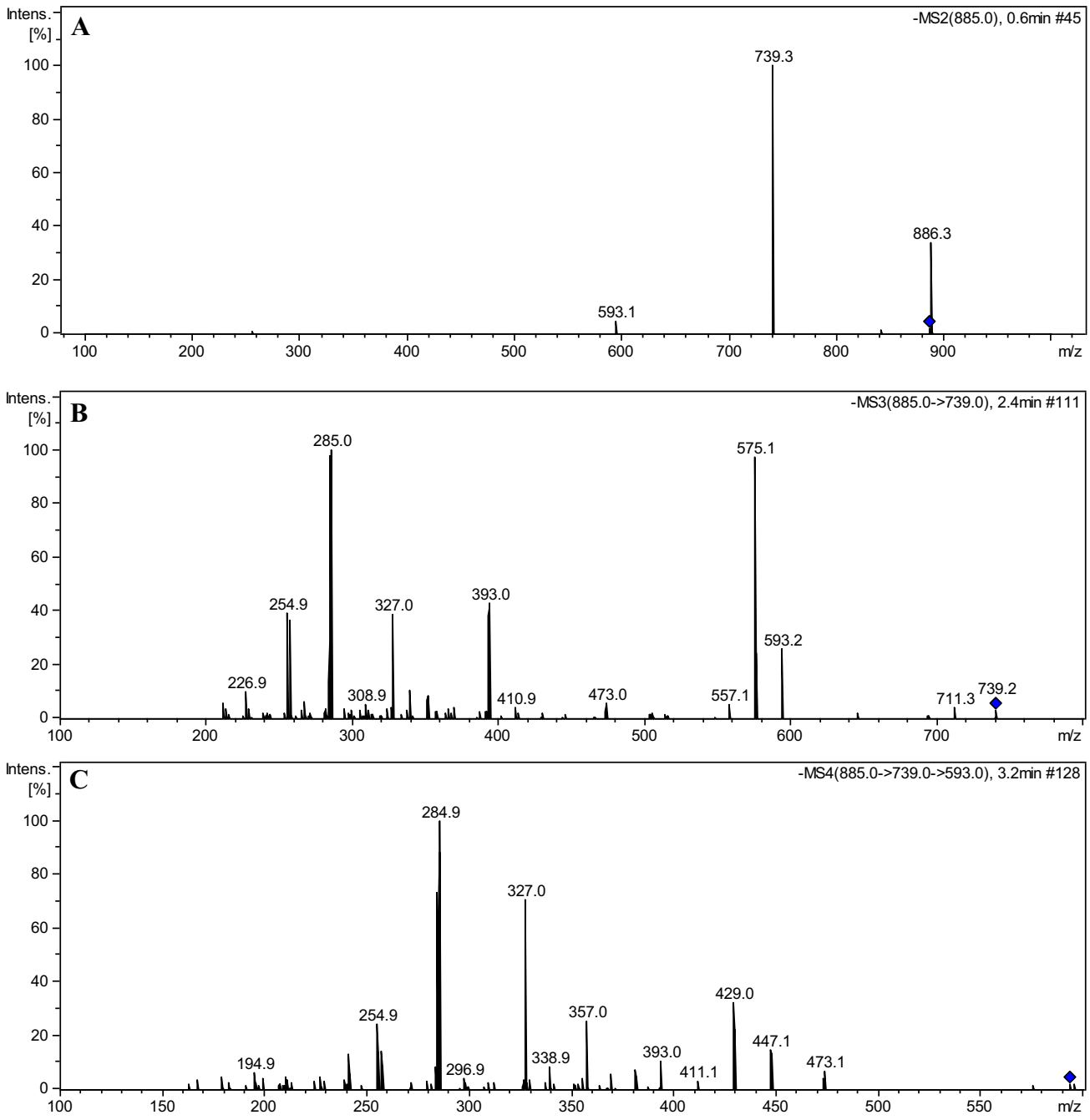

Fig. 2 Mass spectra MS^2 (A), MS^3 (B), and MS^4 (C) of ions *m/z* 885, 739, and 593 referring to flavonoid kaempferol-3-*O*-rhamnosyl-(1→2)-[rhamnosyl-(1→6)]-galactosyl-7-*O*-rhamnoside (**5**).

Compound **5** presented precursor ion *m/z* 885 $[M-H]^-$ and its MS^2 spectrum showed fragment ions *m/z* 739 $[M-H-146]^-$ and 593 $[M-H-292]^-$ indicating the loss of one and two rhamnose units, respectively (Fig. 2A). MS^3 (*m/z* 739) showed the fragment ions *m/z* 593 $[M-H-146]^-$, indicating loss of one rhamnose unit, and 285 $[M-H-454]^-$ suggesting loss of two rhamnose and one hexose units (Fig. 2B). The *m/z* 285 and 255 indicated kaempferol as an aglycone (Fig. 2C and Fig. 8).

Compound **6** presented precursor ion m/z 739 $[M-H]^-$ and its MS^2 spectrum showed the fragment ions m/z 593 $[M-H-146]^-$, indicating loss of one rhamnose, and 285 $[M-H-454]^-$ suggesting loss of two rhamnose and one hexose units (Fig. 3A). The MS^3 (*m/z* 593) presented the fragment ion *m/z* 447 $[M-H-146]^-$ indicating loss of one rhamnose (Fig. 3B), while *m/z* 285 and 255 indicated kaempferol as an aglycone (Fig. 3C and Fig. 8). Hexose, in compounds **5** and **6**, was identified as galactose based on NMR data (Supplementary material), suggested the flavonoids kaempferol-3-*O*-rhamnosyl-(1→2)-[rhamnosyl-(1→6)]-galactosyl-7-*O*-rhamnoside (**5**) and kaempferol-3-*O*-rhamnosyl-(1→6)- galactosyl-7-*O*-rhamnoside (**6**) (Kite, et al., 2007; Silva et al., 2018).

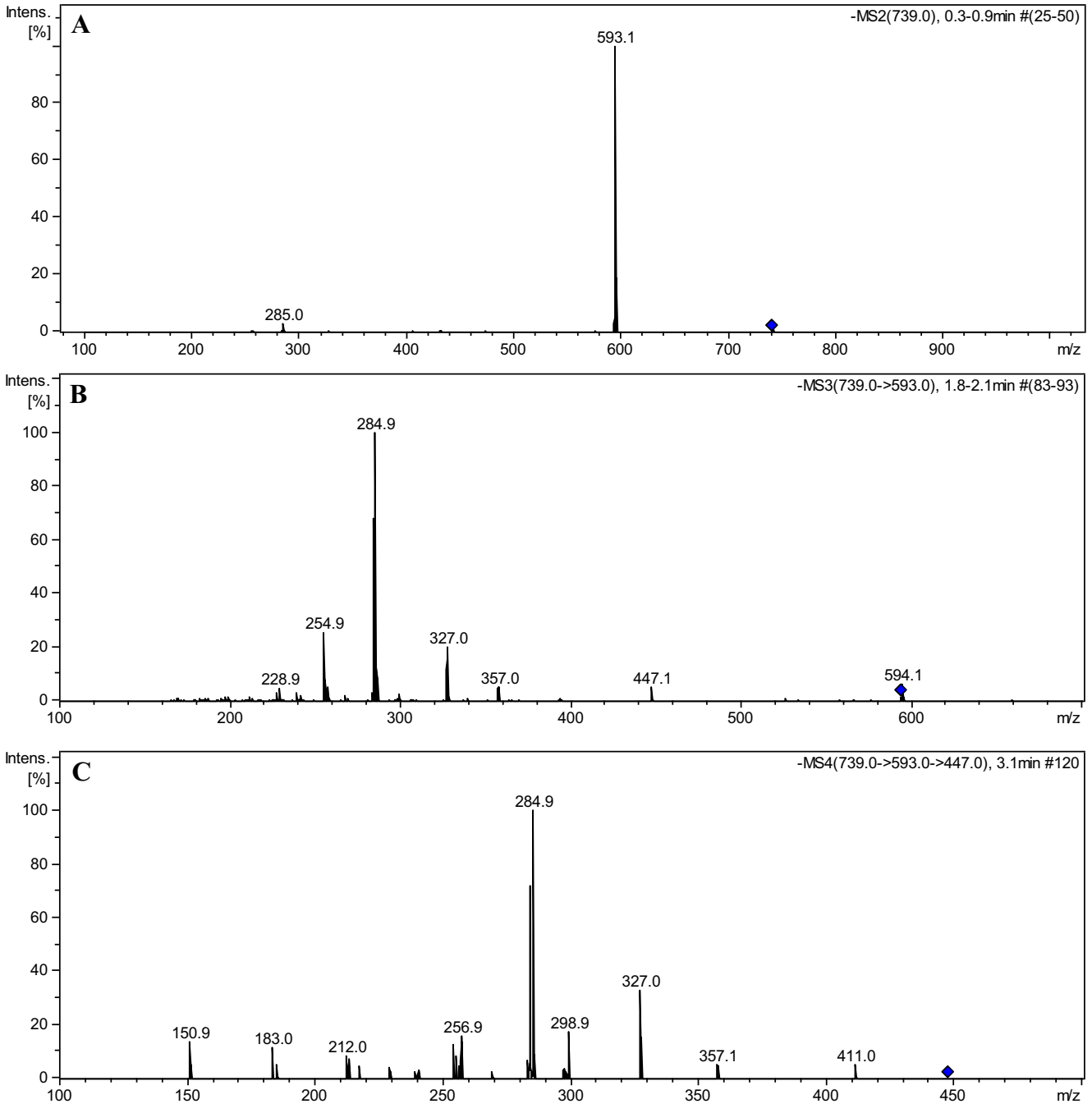

Fig. 3 Mass spectra MS^2 (A), MS^3 (B), and MS^4 (C) of ions *m*/*z* 739, 593, and 447 referring to flavonoid kaempferol-3-*O*-rhamnosyl-(1→6)- galactosyl-7-*O*-rhamnoside (**6**).

Eight flavonols (**1**–**8**), two isoflavonoids (**9** and **10**), and one biflavonoid (**11**) were identified by comparing spectrometric data with scientific literature (Fig. 4 and Table 1). The full scan of the aqueous fraction rich in phenolic compounds is shown in Fig. 5.

The MS^2 spectrum of the precursor ion *m*/*z* 609 $[M-H]^-$ provided the fragment ions *m*/*z* 463 and 301 indicating the consecutive loss of rhamnose (146 Da) and hexose (162 Da) units, respectively, which are characteristic of the quercetin-3-*O*-rhamnosyl-(1→6)-hexoside **(1)**, while the MS^3 of *m*/*z* 301 showed the fragment ions *m*/*z* 283, 271, 255, 179 and 151 confirming quercetin as the aglycone (Fig. 6) (Ablajan et al., 2006).

Two derivatives of quercetin-3-*O*-rhamnosyl-(1→6)-hexoside (**1**) were also identified, corresponding to the precursor ions *m*/*z* 901 $[M-H]^-$ and 755 $[M-H]^-$. The MS^2 spectrum of these ions showed the fragment ion *m*/*z* 609 indicating the loss of two and one rhamnose units, respectively. MS^3 spectrum showed fragmentation identical to that attributed to quercetin-3-*O*-rhamnosyl-(1→6)-hexoside (*m*/*z* 609), suggesting the compound quercetin-3-*O*-rhamnosyl-(1→2)-[rhamnosyl-(1→6)]-hexosyl-7-*O*-rhamnoside (**3**) and quercetin-3-*O*-

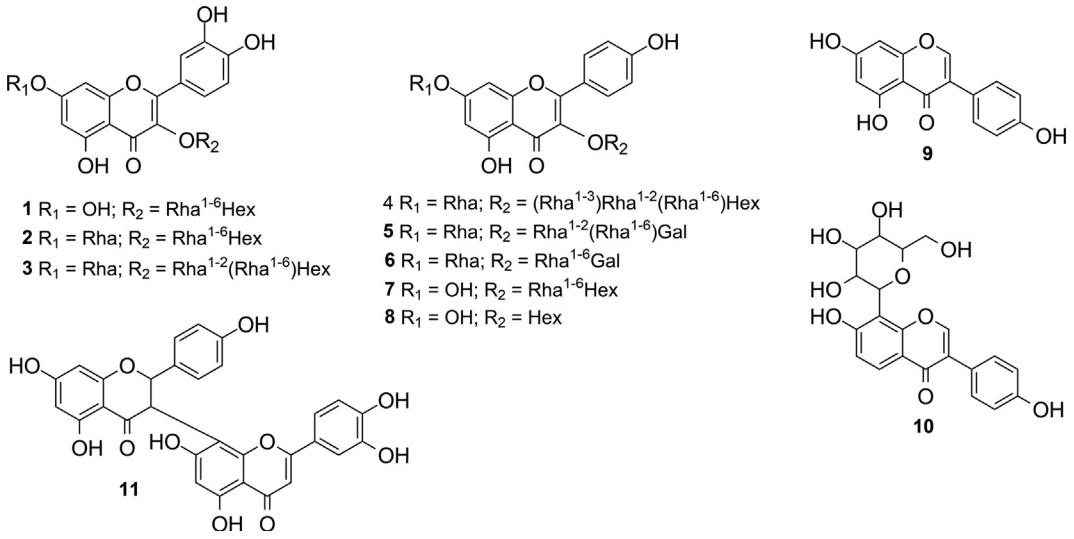

Fig. 4 Structures of the compounds identified in the aqueous fraction of *M. acutifolium* leaves.

Table 1 DI-ESI-MS/MS data for identification of flavonoids in aqueous fraction obtained from *M. acutifolium* (*m*/*z* with relative intensity (%) in parentheses).

Compounds	Molecular Formula	$[M-H]^-$	MS^n	Ref.
quercetin-3-*O*-rhamnosyl-(1→6)-hexoside (**1**)	$C_{27}H_{30}O_{16}$	609	MS^2[609]: 463(13), 301(100) MS^3[301]: 283(24), 271(100), 255(34), 179(98), 151(78)	Ablajan et al., 2006
quercetin-3-*O*-rhamnosyl-(1→6)-hexosyl-7-*O*-rhamnoside (**2**)	$C_{33}H_{40}O_{20}$	755	MS^2[755]: 609(100), 593(7), 447(6) 301 (21), 271(3) MS^3[609]: 593(6), 301(100), 271(23), 227(10)	Crupi et al., 2014
quercetin-3-*O*-rhamnosyl-(1→2)-[rhamnosyl-(1→6)]-hexosyl-7-*O*-rhamnoside (**3**)	$C_{39}H_{50}O_{24}$	901	MS^2[901]: 755(100), 739(6), 609(14) 593(20), 447(2), 301(15) MS^3[755]: 609(26), 593(10), 447(1) 301 (54), 271(30)	Bamawa et al., 2016.
kaempferol-3-*O*-rhamnosyl-(1→3)-rhamnosyl-(1→2)-[rhamnosyl-(1→6)]-hexosyl-7-*O*-rhamnoside (**4**)	$C_{45}H_{60}O_{27}$	1031	MS^2[1031]: 959(23), 885(96), 739(100), 593(3), 575(3), 447(2), 285(4) MS^3[885]: 739(100), 593(3), 575(4), 285(4)	Veitch et al., 2008.
kaempferol-3-*O*-rhamnosyl-(1→2)-[rhamnosyl-(1→6)]-galactosyl-7-*O*-rhamnoside (**5**)	$C_{39}H_{50}O_{23}$	885	MS^2[885]: 739(100), 593(2) MS^3[739]: 593(25), 575(73), 285(100), 255(49)	Bresciani et al., 2015
kaempferol-3-*O*-rhamnosyl-(1→6)-galactosyl-7-*O*-rhamnoside (**6**)	$C_{33}H_{40}O_{19}$	739	MS^2[739]: 593(100), 447(1), 285(3) MS^3[593]: 575(1), 447(4), 285(100), 255(21)	Morchid et al., 2014
kaempferol-3-*O*- rhamnosyl-(1→6)-hexoside (**7**)	$C_{27}H_{30}O_{15}$	593	MS^2[593]: 447(81), 285(100), 284(31), 257(4), 227(10) MS^3[447]: 327(7), 285(100), 255(16)	Crupi et al., 2014
kaempferol-3-*O*-hexoside (**8**)	$C_{21}H_{20}O_{11}$	447	MS^2[447]: 327(7), 285(100), 255(16) MS^3[285]: 255(38), 227(35)	Crupi et al., 2014
genistein (**9**)	$C_{15}H_{10}O_5$	269	MS^2[269]: 241(15), 225(30), 197(25), 143(6)	Zhao et al., 2018
daidzein-8-*C*-glucoside (**10**)	$C_{21}H_{20}O_9$	415	MS^2[415]: 397(13), 379(96), 295(4), 267(19), 249(14)	Ablajan, 2010; Zhao et al., 2018
morelloflavone (**11**)	$C_{30}H_{20}O_{11}$	555	MS^2[555]: 429(100), 403(5) MS^3[429]: 401(100), 295(31)	Carrillo-Hormaza et al., 2016

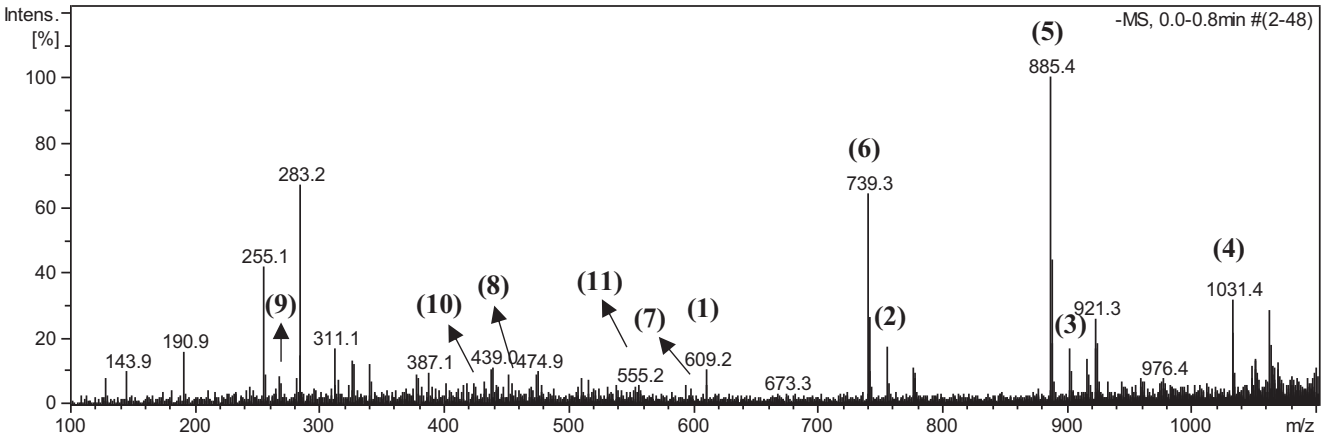

Fig. 5 Full scan DI-ESI-MS/MS $[M-H]^-$ from enriched aqueous fraction, *m/z* 100–1100.

rhamnosyl-(1→6)-hexosyl-7-*O*-rhamnoside **(2)** (Crupi et al., 2014; Bamawa et al., 2016).

The fragmentation pattern of quercetin-3-*O*-rhamnosyl-(1→6)-hexoside **(1)** can be used as a base for the study of other flavonols, including aglycones and their mono- and di-glycosylated derivatives. In the mass spectra of isoflavonoids, a series of regular neutral losses of 28 Da (CO), 44 Da (CO_2), 56 Da (2xCO), 72 Da (CO + CO_2), and 84 Da (3xCO) are generally observed (March et al., 2004; Zhao et al., 2018). These characteristic fragmentations are used to distinguish between flavonols and isoflavonoids.

The MS^2 spectrum of the precursor ion *m/z* 1031 $[M-H]^-$ showed the fragment ions *m/z* 885 $[M-H-146]^-$ and 739 $[M-H-292]^-$ indicating the loss of one and two rhamnose units, respectively. The MS^3 (*m/z* 885) presented the fragment ions *m/z* 739 $[M-H-146]^-$ and 593 $[M-H-292]^-$ indicating loss of one and two rhamnose units, respectively (Fig. 6), while *m/z* 285 and 255 indicated kaempferol as an aglycone, suggesting the flavonoid kaempferol-3-*O*-rhamnosyl-(1→3)-rhamnosyl-(1→2)-[rhamnosyl-(1→6)]-hexosyl-7-*O*-rhamnoside (**4**) (Veitch et al., 2008).

The fragment ions *m/z* 885, 739, 593, and 447 (Fig. 7) are derived from compound **4**, because they show a difference in *m/z* values corresponding to one to four rhamnose units, respectively. This suggests the flavonols kaempferol-3-*O*-rhamnosyl-(1→2)-[rhamnosyl-(1→6)]-galactosyl-7-*O*-rhamnoside (**5**), kaempferol-3-*O*-rhamnosyl-(1→6)-galactosyl-7-*O*-rhamnoside (**6**), kaempferol-3-*O*-rhamnosyl-(1→6)-hexoside

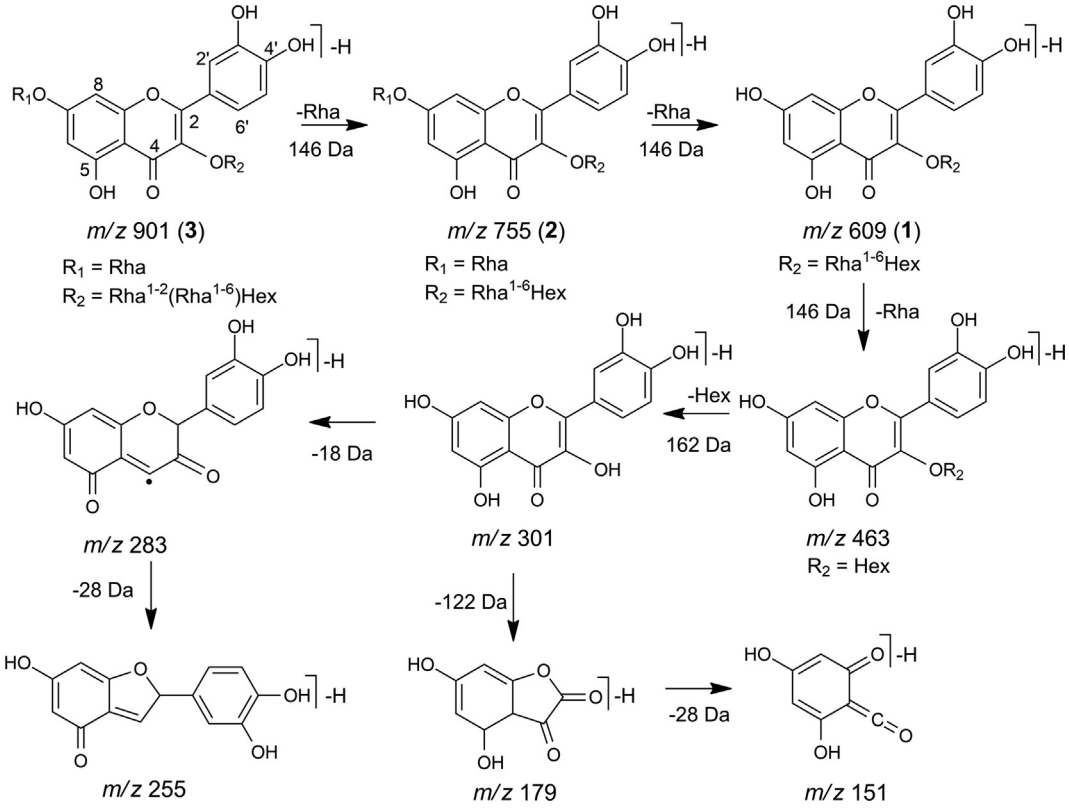

Fig. 6 Fragmentation proposal for flavonoids **1**, **2** and **3**.

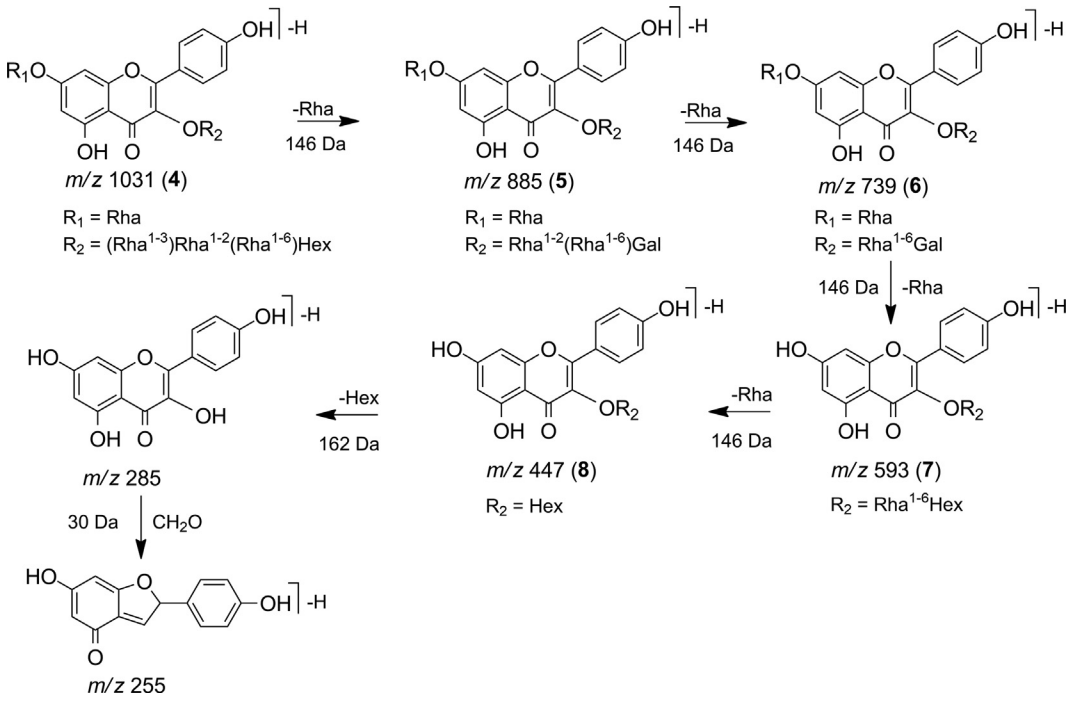

Fig. 7 Fragmentation proposal for flavonoids **4** to **8**.

(**7**) and kaempferol-3-*O*-hexoside (**8**), which is confirmed by the MS^3 of these fragments (Bresciani et al., 2015; Crupi et al., 2014; Morchid et al., 2014), as shown in Table 1.

The fragmentation pattern observed in the MS^2 spectrum of the precursor ion *m/z* 269 $[M-H]^-$ indicates that compound **9** is an aglycone identified as genistein, which can be confirmed by the presence of the fragment ions *m/z* 241 $[M-H-CO]^-$, 225 $[M-H-CO_2]^-$, 197 $[M-H-CO_2-CO]^-$ and 143 $[M-H-C_6H_6O_3]^-$ characteristic of this isoflavonoid. The proposed fragmentation is shown in Fig. 8 (Zhao et al., 2018).

The MS^2 spectrum of *m/z* 415 $[M-H]^-$ showed the fragment ions *m/z* 397 $[M-H-H_2O]^-$ and 379 $[M-H-H_2O-H_2O]^-$ indicating successive water losses that can characterize *C*-glycosylated type isoflavonoids (Zhao et al., 2018). Additionally, the presence of the fragment ions *m/z* 295, 267, and 249 was observed corresponding to the losses of $C_4H_6O_3$, CO, and H_2O, respectively, (Fig. 9), which allowed to suggest the compound daidzein-8-*C*-glucoside (**10**) (Ablajan, 2010; Zhao et al., 2018).

The MS^2 spectrum of the precursor ion *m/z* 555 $[M-H]^-$ showed the fragment ions *m/z* 429 $[M-H-126]^-$ indicating the loss of $-C_6H_6O_3$. The MS^3 (*m/z* 429) presented the fragment ions *m/z* 401 $[M-H-28]^-$ and 295 $[M-H-134]^-$ indicating loss of CO and $C_8H_8O_2$, respectively (Fig. 10), suggesting the biflavonoid morelloflavone (**11**) (Carrillo-Hormaza et al., 2016; Silva et al., 2021).

Some degenerative diseases such as cancer, atherosclerosis, brain dysfunction, as well as many biological complications, including chronic inflammation, *diabetes mellitus*, and autoimmune diseases, are associated with free radicals. The body activates intracellular antioxidant systems in addition to a diet rich in natural antioxidants to control the concentration of these reactive species. Phenolic compounds, especially flavonoids, are powerful antioxidants and potential antidiabetic agents

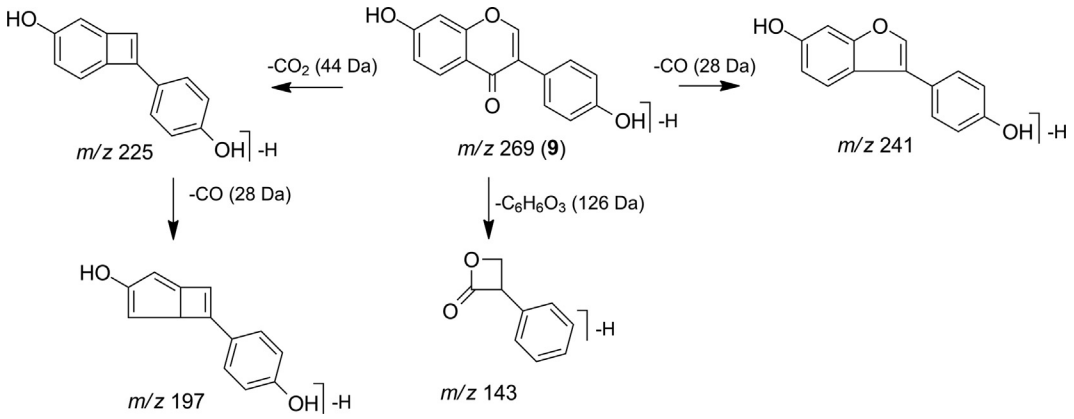

Fig. 8 Fragmentation proposal for genistein (**9**).

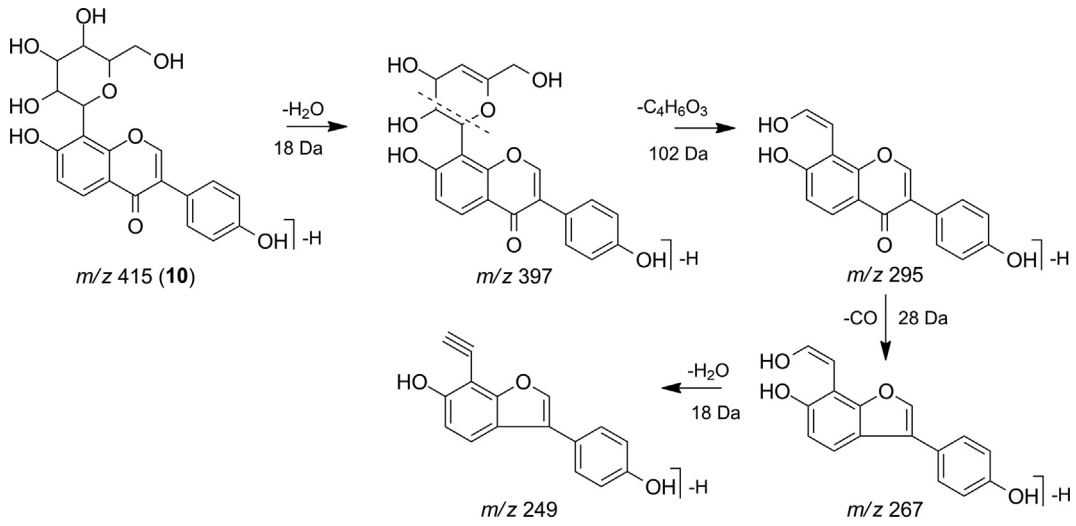

Fig. 9 Fragmentation proposal for daidzein-8-*C*-glucoside (**10**).

(Bursal et al., 2019; Carvalho et al., 2018; Mesa-Vanegas et al., 2015; Taslimi et al., 2020).

The evaluation of the antioxidant activity of the aqueous fraction of *M. acutifolium* in the DPPH assay indicated in the percentage of antioxidant activity of 28.37% ± 0.94 in the concentration of 250 μg mL^{-1}, while for the positive controls BHT and rutin the percentages were 89.88% ± 0.83 and 94.14% ± 0.22, respectively. The total phenolic content (TPC), expressed in mg of gallic acid equivalent per gram of sample (mg of sample/GAE), determined for the aqueous fraction was 151.70 ± 9.44. It is possible to observe the correlation between the percentage of antioxidant activity and the total phenolic content, these data are compatible with the data reported for the extracts from other species *Terminalia brasiliensis* (bark and leaf), *Cenostigma macrophyllum* (leaf) and *Copernicia prunifera* (root) (Sousa et al., 2007).

4. Conclusions

The analyses of the aqueous fraction of *M. acutifolium* leaves by HPLC-DAD suggested the presence of flavonols and isoflavonoids. The study by DI-ESI-MS/MS allowed the identification of the flavonoids quercetin-3-*O*-rhamnosyl-(1→6)-hexoside (**1**), quercetin-3-*O*-rhamnosyl-(1→6)-hexosyl-7-*O*-rhamnoside (**2**), quercetin-3-*O*-rhamnosyl-(1→2)-[rhamnosyl-(1→6)]-hexosyl-7-*O*-rhamnoside (**3**), kaempferol-3-*O*-rhamnosyl-(1→3)-rhamnosyl-(1→2)-[rhamnosyl-(1→6)]-hexosyl-7-*O*-rhamnoside (**4**), kaempferol-3-O-rhamnosyl-(1→2)-[rhamnosyl-(1→6)]-galactosyl-7-*O*-rhamnoside (**5**), kaempferol-3-*O*-rhamnosyl-(1→6)-galacto syl-7-*O*-rhamnoside (**6**), kaempferol-3-*O*-rhamnosyl-(1→6)-hexoside (**7**), kaempferol-3-*O*-hexoside (**8**), the isoflavonoids genistein (**9**), daidzein-8-*C*-glucoside (**10**) and one biflavonoid

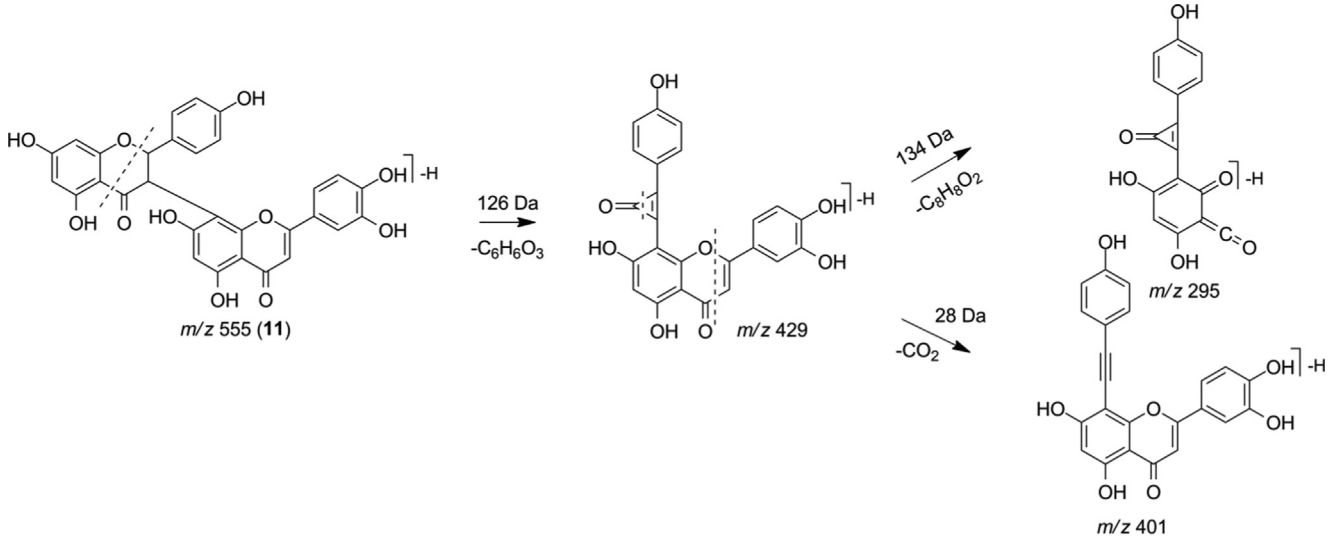

Fig. 10 Fragmentation proposal for morelloflavone (**11**).

morelloflavone (**11**). The structure of flavonoids **5** and **6** was confirmed by NMR. These compounds are being reported for the first time from the leaves of *Machaerium acutifolium*. The percentage of antioxidant activity was lower than the positive controls and the total phenolic content was considered moderate.

Author Contributions

Ruth R. Soares de Farias contributed to the collection and identification of the plant (*Machaerium acutifolium)*. Adonias A. Carvalho, Lucivania R. dos Santos, Jurema S. de Freitas, Renato P. de Sousa, Gerardo M. Vieira Jr. and Mariana H. Chaves contributed in the procedures of the extracts preparation and identification of the compounds. Adonias A. Carvalho also contributed to the draft of the article. Mariana H. Chaves, Gerardo M. Vieira Jr., and Mahendra Rai contributed with revision and critical reading of the manuscript. Mariana H. Chaves and Gerardo M. Vieira Jr. coordinated and supervised the laboratory work. All the authors have read the final manuscript and approved the submission.

Declaration of Competing Interest

The authors declare that they have no known competing financial interests or personal relationships that could have appeared to influence the work reported in this paper.

Acknowledgments

This research was supported by the CAPES and CNPq (PQ-1D: 302470/2018-2, Universal: 406126/2018-6 and INCTBio-Nat: 465637/2014-0). The authors would like to thank for the financial support and scholarships of L. R. Santos, R. P. Sousa, J. S. Freitas, and M. H. Chaves.

Appendix A. Supplementary material

Supplementary data to this article can be found online at https://doi.org/10.1016/j.arabjc.2022.103765.

References

Ablajan, K., 2010. A study of characteristic fragmentation of isoflavonoids by using negative ion ESI-MS^n. J Mass Spectrom. 46 (1), 77–84. https://doi.org/10.1002/jms.1867.

Ablajan, K., Abliz, Z., Shang, X.-Y., He, J.-M., Zhang, R.-P., Shi, J.-G., 2006. Structural characterization of flavonol 3,7-di-*O*-glycosides and determination of the glycosylation position by using negative ion electrospray ionization tandem mass spectrometry. J Mass Spectrom. 41 (3), 352–360. https://doi.org/10.1002/jms.995.

Bamawa, C.M., Ndjele, L.M., Foma, F.M., 2016. Characterization of Leaf Phenolic Compounds of *Sabicea johnstonii* by HPLC-MS^n. J. Nat. Prod. Resour. 2 (2), 86–89.

Barbosa, W.L.R., Pinto, L.N., 2003. Documentação e valorização da fitoterapia tradicional Kayapó nas aldeias A'Ukre e Pykanu - sudeste do Pará. Rev. Bras. Farmacogn. 13, 47–49. https://doi.org/10.1590/S0102-695X2003000300018.

Bresciani, L., Calani, L., Cossu, M., Mena, P., Sayegh, M., Ray, S., Del Rio, D., 2015. (Poly)phenolic characterization of three food supplements containing 36 different fruits, vegetables and berries. Pharma Nutrition. 3 (2), 11–19. https://doi.org/10.1016/j.phanu.2015.01.001.

Bursal, E., Aras, A., Kılıç, Ö., 2019. Evaluation of antioxidant capacity of endemic plant *Marrubium astracanicum* subsp. *macrodon*: Identification of its phenolic contents by using HPLC-MS/MS. Nat. Prod. Res. 33 (13), 1975–1979. https://doi.org/10.1080/14786419.2018.1480018.

Carrillo-Hormaza, L., Ramírez, A.M., Quintero-Ortiz, C., Cossio, M., Medina, S., Ferreres, F., Gil-Izquierdo, A., Osorio, E., 2016. Comprehensive characterization and antioxidant activities of the main biflavonoids of *Garcinia madruno*: A novel tropical species for developing functional products. J. Funct. Foods. 27, 503–516. https://doi.org/10.1016/j.jff.2016.10.001.

Carvalho, A.A., Santos, L.R., Sousa, R.P., Freitas, J.S., Chaves, M. H., 2019. Flavonoids identification of *Machaerium acutifolium* by ESI-MS. In: 7TH BRAZILIAN CONFERENCE ON NATURAL PRODUCT/ XXXIII RESEM PROCEEDINGS, 2019, Rio de Janeiro. Anais eletrônicos... Campinas, Galoá, 2019. Disponível em: < https://proceedings.science/bcnp-2019/papers/flavonoids-identification-of-machaerium-acutifolium-by-esi-ms > Acesso em: 14 jul. 2021.

Carvalho, A.A., Santos, L.R., Farias, R.R.S., Chaves, M.H., Feitosa, C.M., Vieira Júnior, G.M., Araújo, M.R.S., Ferreira, P.M.P., Pessoa, C.O., 2018. Phenolic derivatives and antioxidant activity of polar extracts from *Bauhinia pulchella*. Quim. Nova. 41 (4), 405–411. https://doi.org/10.21577/0100-4042.20170183.

Crupi, P., Genghi, R., Antonacci, D., 2014. In-time and in-space tandem mass spectrometry to determine the metabolic profiling of flavonoids in a typical sweet cherry (*Prunus avium* L.) cultivar from Southern Italy. J Mass Spectrom. 49 (10), 1025–1034. https://doi.org/10.1002/jms.3423.

Es-Safi, N.-E., Kerhoas, L., Einhorn, J., Ducrot, P.-H., 2005. Application of ESI/MS, CID/MS and tandem MS/MS to the fragmentation study of eriodictyol 7-*O*-glucosyl-(1→2)-glucoside and luteolin 7-*O*-glucosyl-(1→2)-glucoside. Int. J. Mass Spectrom. 247 (1–3), 93–100. https://doi.org/10.1016/j.ijms.2005.10.002.

Kite, G.C., Stoneham, C.A., Veitch, N.C., 2007. Flavonol tetraglycosides and other constituents from leaves of *Styphnolobium japonicum* (Leguminosae) and related taxa. Phytochemistry. 68, 1407–1416. https://doi.org/10.1016/j.phytochem.2007.03.004.

Lorenzi, H., 1998. Arvores brasileiras: manual de identificação e cultivo de plantas arbóreas do Brasil, first ed. Plantarum, Nova Odessa, v.2.

Mabry, T.J., Markham, K.R., Thomas, M.B., 1970. The Systematic Identification of Flavonoids. Springer-Verlag, New York.

March, R.E., Miao, X.-S., Metcalfe, C.D., Stobiecki, M., Marczak, L., 2004. A fragmentation study of an isoflavone glycoside, genistein-7-O-glucoside, using electrospray quadrupole time-of-flight mass spectrometry at high mass resolution. Int. J. Mass Spectrom. 232 (2), 171–183. https://doi.org/10.1016/j.ijms.2004.01.001.

Melo, S.J., Sousa, J.P.B., Sá, M.G., Morais, L.S., Magalhães, N.M.G., Gouveia, F.N., Albernaz, L.C., Espindola, L.S., 2021. *Machaerium acutifolium* compounds with larvicidal activity against *Aedes aegypti*. Pest Manag. Sci. 77 (33), 1444–1451. https://doi.org/10.1002/ps.6163.

Mesa-Vanegas, A.M., Zapata-Uribe, S., Arana, L.M., 2015. Actividad antioxidante de extractos de diferente polaridad de *Ageratum conyzoides* L. Bol. Latinoam. Caribe Plant. Med. Aromat. 14 (1), 1–10.

Morchid, E.M.E., Londoño, P.T., Papagiannopoulos, M., Gobbo-Neto, L., Müller, C., 2014. Variation in flavonoid pattern in leaves and flowers of *Primula veris* of different origin and impact of UV-B. Biochem. Syst. Ecol. 53, 81–88. https://doi.org/10.1016/j.bse.2013.12.032.

Ollis, W.D., Redman, B.T., Sutherland, I.O., Gottlieb, O.R., 1978. Petrostyrene, a cinnamylphenol from *Machaerium acutifolium*. Phytochemistry. 17, 1379–1381. https://doi.org/10.1016/S0031-9422(00)94593-X.

Pinheiro, P. F., Justino, G. C., 2012. Structural Analysis of Flavonoids and Related Compounds - A Review of Spectroscopic Applications

in: Rao, V. (Ed), Phytochemicals - A Global Perspective of Their Role in Nutrition and Health, InTechOpen, pp. 33-56. ISBN: 978-953-51-0296-0. https://www.intechopen.com/books/phytochemicals-a-global-perspective-of-their-role-in-nutrition-and-health/structural-analysis-of-flavonoids-and-related-compounds-a-review-of-spectroscopic-applications.

Polido, C.A., Sartori, A.L.B., 2007. O gênero *Machaerium* (Leguminosae-Papilionoideae-Dalbergieae) no pantanal brasileiro. Rodriguésia. 58 (2), 313–329. https://doi.org/10.1590/2175-7860200758208.

Prasain, J.K., Patel, R., Kirk, M., Wilson, L., Botting, N., Darley-Usmar, V.M., Barnes, S., 2003. Mass spectrometric methods for the analysis of chlorinated and nitrated isoflavonoids: a novel class of biological metabolites. J. Mass Spectrom. 38 (7), 764–771. https://doi.org/10.1002/jms.492.

Silva, A.G.A., Moreira, R.A., Sousa, R.P., Filho, E.S.M., Veras, M.D. A., Chaves, M.H., Freitas, S.D.L., 2021. Composição química e atividades fotoprotetora e antiradicalar in vitro dos galhos de *Platonia insignis* (Clusiaceae). Quim. Nova. 44 (8), 954–962. https://doi.org/10.21577/0100-4042.20170761.

Silva, L.M.P., Alves, J.S.F., Siqueira, E.M.S., Souza Neto, M.A., Abreu, L.S., Tavares, J.F., Porto, D.L., Ferreira, L.S., Demarque, D.P., Lopes, N.P., Aragão, C.F.S., Zucolotto, S.M., 2018. Isolation and identification of the five novel flavonoids from *Genipa americana* leaves. Molecules. 23 (10), 1–13. https://doi.org/10.3390/molecules23102521.

Sousa, C.M.M., Silva, H.R., Vieira-Júnior, G.M., Ayres, C.C., Costa, L.S., Araújo, D.S., Cavalcante, L.C.D., Barros, E.D.S., Araújo, P. B.M., Brandão, M.S., Chaves, M.H., 2007. Fenóis totais e atividade antioxidante de cinco plantas medicinais. Quim. Nova. 30 (2), 351–355. https://doi.org/10.1590/S0100-40422007000200021.

Taslimi, P., Köksal, E., Gören, A.C., Bursal, E., Aras, A., Kılıç, Ö., Alwasel, S., Gülçin, İ., 2020. Anti-Alzheimer, antidiabetic and antioxidant potential of *Satureja cuneifolia* and analysis of its phenolic contents by LC-MS/MS. Arab. J. Chem. 13 (3), 4528–4537. https://doi.org/10.1016/j.arabjc.2019.10.002.

Veitch, N.C., Kite, G.C., Lewis, G.P., 2008. Flavonol pentaglycosides of *Cordyla* (Leguminosae: Papilionoideae: Swartzieae): Distribution and taxonomic implications. Phytochemistry. 69, 2329–2335. https://doi.org/10.1016/j.phytochem.2008.05.026.

Vukics, V., Guttman, A., 2010. Structural characterization of flavonoid glycosides by multi-stage mass spectrometry. Mass Spectrom. Rev. 29 (1), 1–16. https://doi.org/10.1002/mas.20212.

Zhao, W., Shang, Z., Li, Q., Huang, M., He, W., Wang, Z., Zhang, J., 2018. Rapid Screening and Identification of Daidzein Metabolites in Rats Based on UHPLC-LTQ-Orbitrap Mass Spectrometry Coupled with Data-Mining Technologies. Molecules. 23 (1), 1–24. https://doi.org/10.3390/molecules23010151.